Atmospheric Research 249 (2021) 105363

Contents lists available at ScienceDirect

Atmospheric Research

journal homepage: www.elsevier.com/locate/atmosres

Co-occurrence of ozone and $PM_{2.5}$ pollution in the Yangtze River Delta over 2013–2019: Spatiotemporal distribution and meteorological conditions

Huibin Dai, Jia Zhu, Hong Liao *, Jiandong Li, Muxue Liang, Yang Yang, Xu Yue

Jiangsu Key Laboratory of Atmospheric Environment Monitoring and Pollution Control, Jiangsu Collaborative Innovation Center of Atmospheric Environment and Equipment Technology, School of Environmental Science and Engineering, Nanjing University of Information Science & Technology, Nanjing 210044, China

ARTICLE INFO

Keywords:
Co-occurrence
Ozone and $PM_{2.5}$
Pollution
Typical weather patterns

ABSTRACT

We examined the spatial-temporal variations of surface-layer ozone (O_3) and $PM_{2.5}$ (particulate matter with an aerodynamic equivalent diameter of 2.5 μm or less) observed from April 2013 to December 2019 in the Yangtze River Delta (YRD) region to identify the O_3-$PM_{2.5}$ relationship and to focus on the co-polluted days by O_3 and $PM_{2.5}$. Averaged over the YRD, the observed annual mean concentration of maximum daily 8 h average ozone (MDA8 O_3) increased by 36.8 μg m^{-3} (49.5%) whereas that of $PM_{2.5}$ decreased by 13.3 μg m^{-3} (22.1%) over 2014–2019. During warm months of April-October of 2013–2019, the observed regional mean daily concentrations of MDA8 O_3 and $PM_{2.5}$ had a small positive correlation of 0.23, and this correlation coefficient became 0.44 when the long term trends were removed from the concentrations. The days with co-pollution of MDA8 O_3 and $PM_{2.5}$ (MDA8 $O_3 > 160$ μg m^{-3} and $PM_{2.5} > 75$ μg m^{-3}) were observed frequently, which reached 54 days in Shanghai and 71 days in Jiangsu province during 2013–2019. Such co-polluted days in the YRD were found to occur mainly in the months of April, May, June, and October. The occurrence of co-pollution in the YRD is found to be mainly dependent on relative humidity, surface air temperature, and wind speed. The mean anomalous values of these three variables were, respectively, −7.3%, 0.46 °C, −0.17 m s^{-1} for days with O_3 pollution alone while −6.2%, 1.84 °C, and −0.40 m s^{-1} for days with co-pollution. Four typical weather patterns were identified to be associated with the co-polluted days. Our results provide better understanding of the complex air pollution and have implications for the control of such co-polluted events.

1. Introduction

Tropospheric ozone (O_3) and $PM_{2.5}$ (particulate matter with an aerodynamic equivalent diameter of 2.5 μm or less) are major air pollutants in the atmosphere that have adverse effects on human health (Gao and Ji, 2018; Xie et al., 2019; Jiang et al., 2019), crops (Wang et al., 2005; Wang et al., 2007) and plants (Ren et al., 2011; Yue et al., 2017). They have also made significant contributions to climate change since pre-industrial times (Stocker et al., 2013). Ground-level O_3 is produced by photochemical reactions of nitrogen oxides (NO_x) and volatile organic compounds (VOCs) in the presence of intense ultraviolet light (Xue et al., 2014). $PM_{2.5}$ is composed of primary aerosols (such as black carbon, primary organic carbon, mineral dust) and secondary aerosols (such as sulfate, nitrate, ammonium, and secondary organic carbon). Concentrations of tropospheric O_3 and $PM_{2.5}$ are coupled through the formation and growth of aerosols, heterogeneous reactions, and aerosol-induced changes in photolysis rates (Lou et al., 2014). Since 2013, the governmental "Air Pollution Prevention and Control Action Plan" (hereafter called "Action Plan") has been implemented to improve air quality in China. Thanks to the strict emission abatements, $PM_{2.5}$ concentrations in China have decreased significantly (Zhang et al., 2018a). However, current concentrations of $PM_{2.5}$ still frequently exceed the national air quality standard, and O_3 pollution is getting worse (Li et al., 2019b). Examining the relations between O_3 and $PM_{2.5}$ since the "Action Plan" is essential for the coordinated control of these two pollutants.

As one of the major urban agglomerations in China, the Yangtze River Delta (YRD) region is located in the eastern part of China's mainland. It is the largest economic zone with high anthropogenic and biogenic emissions. Over the YRD in 2014, the anthropogenic SO_2 and NO_x emissions were estimated to be 2.0×10^6 ton yr^{-1} and 8.9×10^5 ton yr^{-1} (Sha et al., 2019), respectively, and the BVOCs (biogenic volatile organic compounds) emissions were 1.9×10^6 ton yr^{-1} (Liu et al., 2018). Air quality in the YRD can also be influenced by the transport of pollutants from the North China Plain (Sun et al., 2017).

* Corresponding author.
E-mail address: hongliao@nuist.edu.cn (H. Liao).

https://doi.org/10.1016/j.atmosres.2020.105363
Received 27 September 2020; Received in revised form 8 November 2020; Accepted 10 November 2020
Available online 13 November 2020

Previous studies have examined the spatial-temporal variations of O_3 pollution over the YRD (Xu et al., 2008; Yu et al., 2019; Li et al., 2019a). By analyzing the observations in Lin'an, a background site in the YRD, Xu et al. (2008) found that the average of the monthly highest 5% MDA8 O_3 (maximum daily 8 h average ozone) concentrations increased at a rate of 0.68 ppbv yr^{-1} over years of 1991–2006. Yu et al. (2019) analyzed the observed MDA8 O_3 concentrations from Ministry of Ecology and Environment (MEE) and found that the increasing trends of MDA8 O_3 in most cities in the YRD were in the range of 1.35–8.14 μg m^{-3} yr^{-1} over the years of 2013–2017. Li et al. (2019a) reported that the 5 yr (2013–2017) averages of observed summertime MDA8 O_3 at sites in the YRD were as high as 50–80 ppbv and the decreases in NO_x emissions increased O_3 levels in the urban areas of the YRD.

The distributions and variations of $PM_{2.5}$ concentrations in the YRD have also been examined (Shu et al., 2017; Zhang et al., 2018a; Hou et al., 2019). Shu et al. (2017) analyzed observed daily $PM_{2.5}$ concentrations from MEE in sixteen cities of the YRD during December 2013 to November 2014, and found that $PM_{2.5}$ concentrations were relatively higher in inland cities of the YRD, because the coastal cities of the YRD were most likely influenced by clean marine air masses. Zhang et al., 2018a examined the observed $PM_{2.5}$ concentrations from January 2013 to December 2017 from MEE and revealed that the annual mean $PM_{2.5}$ concentrations in the YRD dropped by 33.7% since the implementation of the "Action Plan". Hou et al. (2019) reported, on the basis of the observed $PM_{2.5}$ concentrations from MEE, that the mean $PM_{2.5}$ concentration in the YRD during 2013–2018 was 50.5 μg m^{-3} and the most severe $PM_{2.5}$ pollution in the YRD occurred in winter under stagnant weather conditions.

Few previous studies were focused on the O_3-$PM_{2.5}$ relationships and the meteorological conditions favorable for the co-occurrence of high levels of $PM_{2.5}$ and O_3. Ding et al. (2013) analyzed 1 yr (August 2011–July 2012) hourly measurements of O_3 and $PM_{2.5}$ at the Station for Observing Regional Processes of the Earth System (SORPES) in Nanjing and found a positive correlation between concentrations of secondary fine particles ($PM_{2.5}$) and those of O_3 in summer, indicating enhanced conversion of SO_2 to sulfate with high concentrations of oxidants. Wang et al. (2014) analyzed daily concentrations of $PM_{2.5}$, PM_{10}, CO, SO_2, NO_2, and O_3 from MEE in the 31 provincial capital cities during March 2013–February 2014, and found a weak positive correlation ($0 < r \leq 0.25$) between daily concentrations of O_3 and $PM_{2.5}$ in the YRD. Zhu et al. (2019) examined the spatial-temporal characteristics of the correlations between observed $PM_{2.5}$ and O_3 from MEE at 1497 sites for 2016 and found that concentrations of $PM_{2.5}$ were positively correlated with those of O_3 in summer in the YRD. These studies examined O_3–$PM_{2.5}$ relationship for a short period of about a year. No previous studies, to our knowledge, have examined the co-occurrence of O_3 and $PM_{2.5}$ pollution as well as the meteorological factors and predominant synoptic weather patterns for such co-pollution days.

This study aims to: 1) examine the temporal trends and spatial variations of MDA8 O_3 and $PM_{2.5}$ concentrations in the YRD, with a special focus on the relations between MDA8 O_3 and $PM_{2.5}$, by analyzing the hourly concentrations measured at the monitoring sites in the YRD for years 2013–2019, and 2) identify the meteorological factors and predominant synoptic weather patterns favorable for co-occurrence of O_3 and $PM_{2.5}$ pollution. The methods, including the descriptions of studied area, in situ measurements, and data analysis are presented in Section 2. Section 3 shows the results, including the spatial-temporal variations of MDA8 O_3 and $PM_{2.5}$ in the YRD during 2013–2019, the MDA8 O_3-$PM_{2.5}$ relationship, as well as the favorable meteorological factors and synoptic weather patterns for co-pollution days. The conclusions are presented in Section 4.

2. Methods

2.1. Studied area

The Yangtze River Delta urban agglomeration is located at 29.3°N to 32.6°N latitude and 115.8°E to 123.4°E longitude. The spatial distributions of cities in the YRD with measurements of pollutants are shown in Fig. 1. Twenty-five cities are considered, including Shanghai, 9 cities (Nanjing, Wuxi, Changzhou, Suzhou, Nantong, Yancheng, Yangzhou, Zhenjiang, Taizhou) in Jiangsu Province, 7 cites (Hangzhou, Ningbo, Jiaxing, Shaoxing, Jinhua, Zhoushan, Taizhou) in Zhejiang Province, and 8 cities (Hefei, Wuhu, Maanshan, Tongling, Anqing, Zhangzhou, Chizhou, Xuancheng) in Anhui Province.

2.2. Observed concentrations of air pollutants and meteorological parameters

Hourly concentrations of $PM_{2.5}$ and O_3 in 25 cities during years of 2013–2019 are taken from the public website of MEE (beijingair.sinaapp.com/). Note that we collected the observational network data starting from April 2013. The measurements have been widely used in previous studies (Zhu et al., 2019; Li et al., 2019b; Hou et al., 2019). According to the Chinese National Ambient Air Quality Standard (NAAQS), concentrations of MDA8 O_3 (or daily mean $PM_{2.5}$) are above the Grade II air quality standard if concentrations are higher than 160 μg m^{-3} (or 75 μg m^{-3}). We pay special attentions to the co-pollution days when concentrations of both MDA8 O_3 and $PM_{2.5}$ are above the Grade II standards.

The surface daily meteorological parameters used in this study, such as wind speed (WS), relative humidity (RH) and surface air temperature (TS), are taken from the China Meteorological Science Data Sharing Service Network (http://data.cma.cn/ data/cdcdetail/dataCode/SURF_CLI_CHN_MUL_DAY_V3.0.html). Meteorological data are available for 13 cities in the YRD (Fig. 1), including Shanghai, Nanjing, Zhenjiang, Nantong, Wuxi, Hangzhou, Zhoushan, Jinhua, Taizhou, Hefei, Chizhou, Ma'anshan, and Tongling.

To analyze the synoptic weather patterns, we also use fields of geopotential height, winds, temperature, and relative humidity from the National Center for Environmental Prediction (NCEP)/National Center for Atmospheric Research (NCAR) global reanalysis datasets at a resolution of 2.5° latitude by 2.5° longitude.

2.3. Data analyses

We examine O_3-$PM_{2.5}$ relationship by using daily concentrations. Following the NAAQS, the daily mean $PM_{2.5}$ concentration is calculated when there are valid data for more than 20 h during that day and the 8 h average O_3 concentration is calculated when there are valid data for at least 6 h for each 8 h.

For the purpose of examining the relationship between daily MDA8 O_3 and daily $PM_{2.5}$ for April-October of 2013–2019, the long term trends of $PM_{2.5}$ and MDA8 O_3 have to be removed, otherwise the observed decreases in $PM_{2.5}$ and increases in O_3 over 2013–2019 would produce negative O_3-$PM_{2.5}$ correlations (Li et al., 2019b). Besides, the monthly variations of $PM_{2.5}$ and MDA8 O_3 from April to October should also be removed. Therefore, we used the detrended and deseasonalized concentrations to examine O_3-$PM_{2.5}$ relationship and the co-pollution on daily basis. The similar method has also been used in the study of Tai et al. (2010), the deviations of MDA8 O_3 (Dev_MDA8 O_3) and $PM_{2.5}$ (Dev_$PM_{2.5}$) are calculated by:

$Dev_{mi} = C_{mi} - \sum_{i=1}^{n} \frac{C_{mi}}{n}$ where C_{mi} is the MDA8 O_3 ($PM_{2.5}$) concentration on day i in month m, n is the number of days in month m, and $\sum_{i=1}^{n} \frac{C_{mi}}{n}$ represents the average concentration in month m. Therefore, the positive Dev_{mi} indicates that the MDA8 O_3 ($PM_{2.5}$) concentration on day i is higher than the monthly mean value for that month m (within which

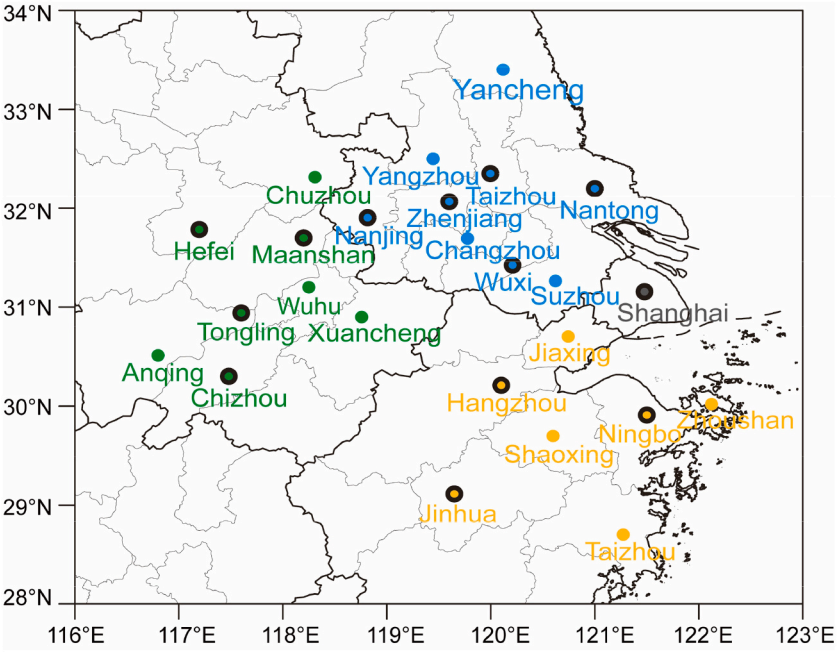

Fig. 1. Spatial distribution of cities with observed concntrations of pollutants in the Yangtze River Delta region (including Anhui province (colored green), Jiangsu province (blue), Zhejiang province (yellow), and Shanghai (grey)). The dots with black circles indicate the 13 cities with also observed meteorological data available.

the sample is collected).

3. Results

3.1. Simultaneous variations of concentrations of MDA8 O_3 and $PM_{2.5}$ in the YRD

The spatial distributions of annual mean concentrations of MDA8 O_3 and $PM_{2.5}$ in the YRD in each year of 2014–2019 are shown in Figs. 2 (a) and 2 (b), respectively. Note year 2013 is not shown becuase the observations in that year started from April. For MDA8 O_3, the annual and regional mean concentration in the YRD increased from 74.4 μg m^{-3} in 2014 to 111.2 μg m^{-3} in 2019, which was an increase of 36.8 μg m^{-3} (49.5%) over the studied time period. In the mean time, the annual and regional mean concentration of $PM_{2.5}$ in the YRD exhibited a large decrease of 13.3 μg m^{-3} (22.1%) (from 60.1 μg m^{-3} in 2014 to 46.8 μg m^{-3} in 2019), but the annual mean $PM_{2.5}$ concentrations in most cities in 2019 still exceeded the Grade I standard (i.e., 35 μg m^{-3}) of the NAAQS, indicating the severity of the current $PM_{2.5}$ pollution in the YRD. Averaged over the YRD, over 2014–2019, annual mean concentrations of O_3 and $PM_{2.5}$ exhibited trends of 7.3 μg m^{-3} yr^{-1} and -3.3 μg m^{-3} yr^{-1}, respectively. The reductions in $PM_{2.5}$ contributed to the increases in MDA8 O_3 concentrations, because $PM_{2.5}$ scavenges the chemical radicals that would otherwise produce O_3 (Li et al., 2019b, Liu and Wang, 2020).

Fig. 2(c) shows the monthly variations in MDA8 O_3 and $PM_{2.5}$ concentrations averaged over the cities in the YRD for each year of 2013–2019. High concentrations of MDA8 O_3 mainly occurred from April to October; on the contrary, $PM_{2.5}$ concentrations exhibited the highest values from November to February. It is noted that $PM_{2.5}$ concentrations exceeded Grade I standard of the NAAQS even in the warm seasons. While the stagnant weather conditions and high emissions together lead to severe $PM_{2.5}$ pollution in winter (Cai et al., 2017; Zhang et al., 2018b), the strong solar radiation and high temperatures are conducive to photochemical reactions and O_3 production in warm seasons (Wang et al., 2018a; Gong and Liao, 2019). The slight decreases in MDA8 O_3 and the low concentrations of $PM_{2.5}$ in June and July were attributed to the East Asian summer monsoon, which led to cloudy and rainy weather conditions in the YRD and influenced photochemical reactions and wet deposition of pollutants (Ding et al., 2013; Wang et al., 2018b).

The trends in seasonal and annual mean concentrations of MDA8 O_3 and $PM_{2.5}$ are further investigated (Figs. S1(a) and S1(b) in the supplementary material). Over 2014–2019, MDA8 O_3 concentrations in most cities in the YRD exhibited an increasing trend, with the largest increases in March-April-May (MAM) and June-July-August (JJA) when photochemical reactions are strong. The maximum trend of +17.8 μg m^{-3} yr^{-1} occurred in Chuzhou in MAM. MDA8 O_3 concentrations in December-January-February (DJF) also exhibited increasing trends, with the highest trend of +6.7 μg m^{-3} yr^{-1} in Suzhou. Over the same years, $PM_{2.5}$ concentrations in all seasons exhibited decreasing trends in almost all cities in the YRD, except that a couple of cities (for example, Chizhou, Zhenjiang, and Yangzhou in MAM) had small increasing trends. Benefited from the "Action Plan", $PM_{2.5}$ pollution in DJF in the YRD was abated significantly, with the largest drop of 9.4 μg m^{-3} yr^{-1} in Nanjing.

Figs. 3 (a) and 3(b) show the numbers of polluted days with concentrations of MDA8 O_3 or $PM_{2.5}$ exceeded the Grade II standards of NAAQS over 2013–2019 in the YRD. The largest number of polluted days for MDA8 O_3 ($PM_{2.5}$) was 363 (708) days in Jiaxing in Zhejiang province (in Hefei in Anhui province) of the YRD. As shown in Fig. 3 (c), the numbers of co-polluted days were the highest (exceeding 45 days) in Shanghai and in 4 cities (Nantong, Taizhou, Yangzhou, and Zhenjiang) in Jiangsu province, which could be caused by high anthropogenic emissions in this region (sha et al., 2019). Fig. S2 shows the percentages of different polluted days in total days of 2013–2019. The highest percentages of O_3 polluted days, $PM_{2.5}$ polluted days and the co-polluted days among the total days reached 14.7% in Jiaxing of Zhejiang province, 44.7% in Hefei of Anhui province, and 3.4% in Taizhou of Jiangsu province, respectively. As for the interannual changes of these polluted days, from 2014 to 2019, shown in Fig. S3, most cities in the YRD exhibited increases in O_3 polluted days and decreases in $PM_{2.5}$ polluted days as well as the co-polluted days, indicating the importance of controlling O_3 and $PM_{2.5}$ pollution simultaneously.

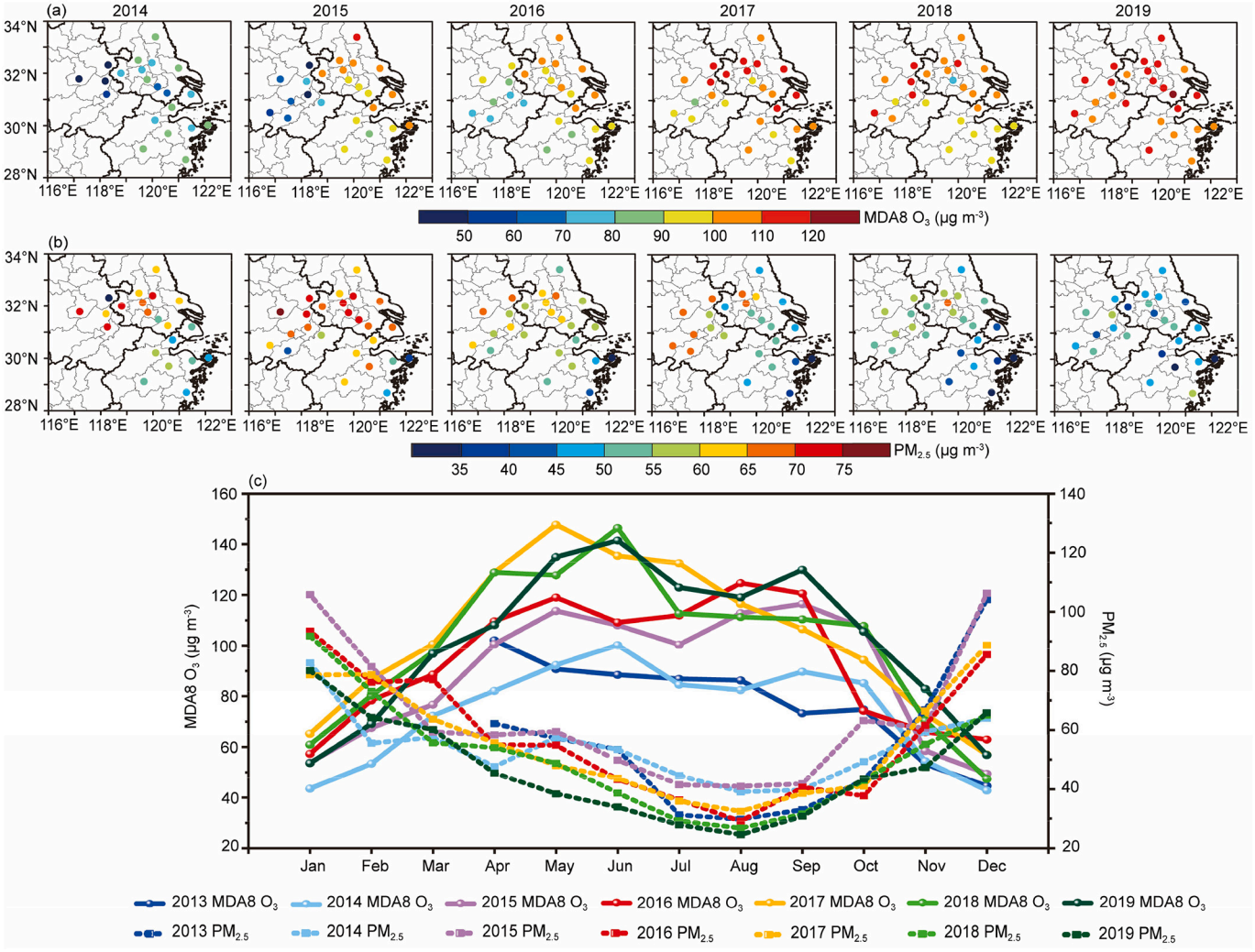

Fig. 2. The spatial distributions of (a) annual mean MDA8 O_3 concentrations (μg m^{-3}) and (b) annual mean $PM_{2.5}$ concentrations (μg m^{-3}) in YRD for years of 2014–2019. (c) Monthly variations of MDA8 O_3 and $PM_{2.5}$ concentrations (μg m^{-3}) averaged over YRD, from April 2013 to December 2019.

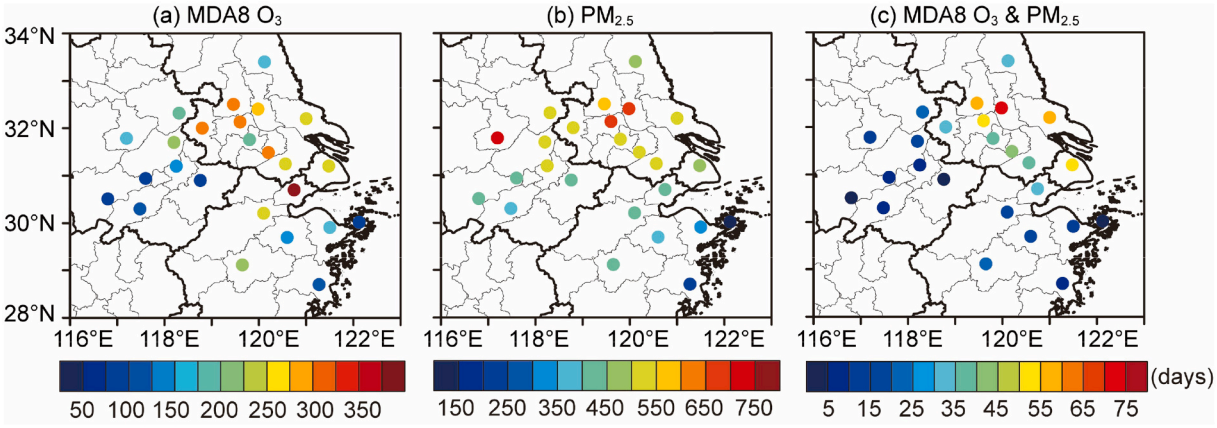

Fig. 3. Numbers of polluted days with (a) MDA8 O_3 exceeded NAAQS Grade II standard (daily MDA8 O_3 > 160 μg m^{-3}), (b) $PM_{2.5}$ exceeded NAAQS Grade II standard (daily mean $PM_{2.5}$ > 75 μg m^{-3}), and (c) both MDA8 O_3 and $PM_{2.5}$ exceeded NAAQS Grade II standard during 2013–2019 in YRD.

3.2. *Relationships between MDA8 O_3 and $PM_{2.5}$ in the YRD*

We examine the relations between daily MDA8 O_3 and $PM_{2.5}$ for months of April-October when O_3 concentrations were high. The daily concentrations of MDA8 O_3 and $PM_{2.5}$ averaged over the YRD are shown in Figs. 4(a) and 4(b), respectively, for April-October of 2013–2019. The linear trends indicate that concentrations of MDA8 O_3 increased and those of $PM_{2.5}$ decreased over 2013–2019. The correlation coefficient between daily MDA8 O_3 and daily $PM_{2.5}$ was 0.23 (statistically significant at the 95% level) as concentrations are averaged over the YRD. For

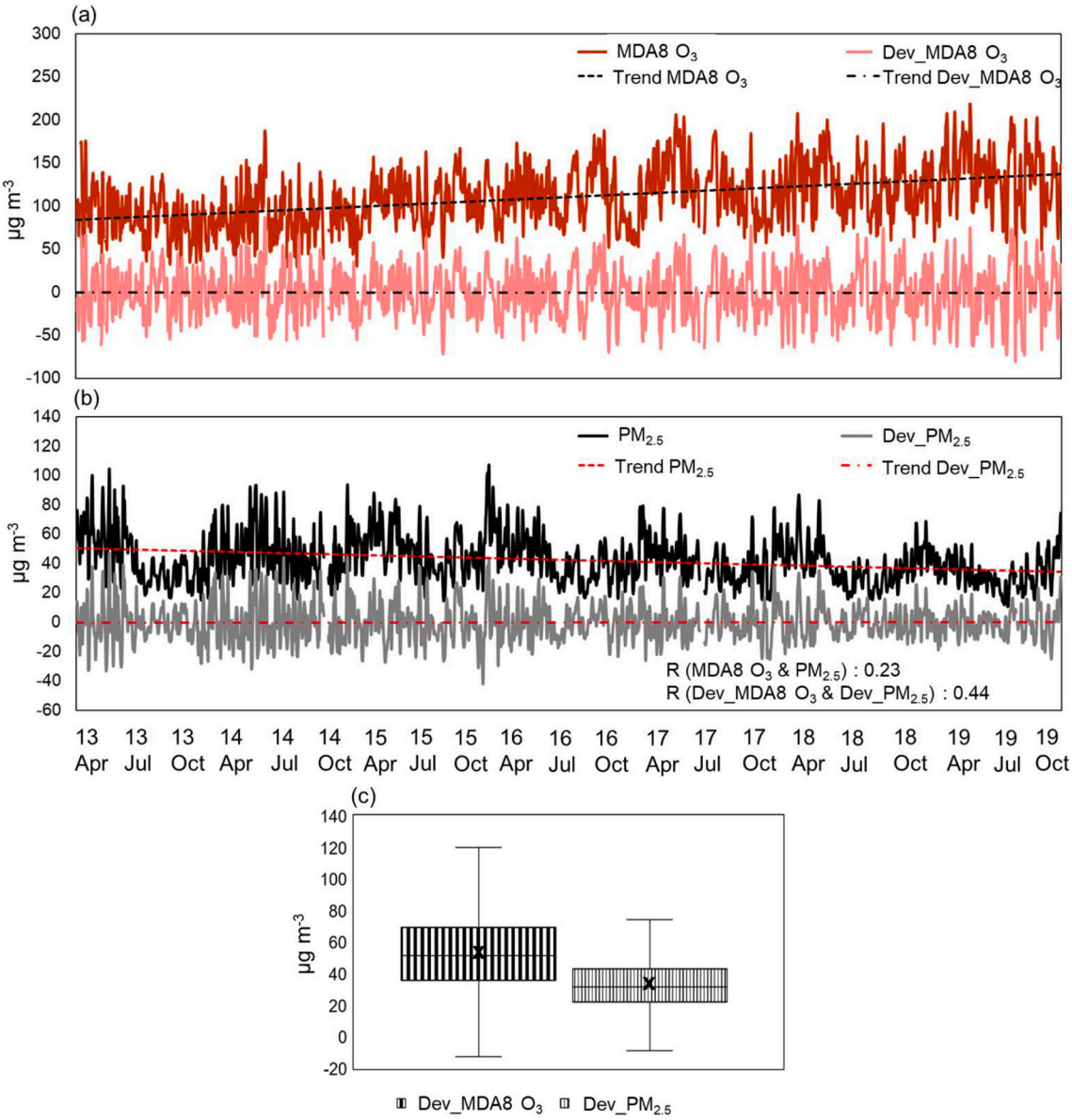

Fig. 4. Daily concentrations (μg m^{-3}) of (a) MDA8 O_3 and Dev_MDA8 O_3, (b) $PM_{2.5}$ and Dev_$PM_{2.5}$ for April-October of 2013–2019. All the concentrations are averaged over YRD. (c) The boxplot of Dev_MDA8 O_3 (Dev_$PM_{2.5}$) during MDA8 O_3 ($PM_{2.5}$) exceedance days in 25 cities with 4869 (2598) samples from April to October during 2013–2019. The boxes enclose the 25th, 50th and 75th percentile, the whiskers represent the 5th and 95th percentile, the crosses represent the average values.

the purpose of examining daily O_3-$PM_{2.5}$ relationship, the deviations of MDA8 O_3 (Dev_MDA8 O_3) and $PM_{2.5}$ (Dev_$PM_{2.5}$) are calculated to remove monthly variations and multi-year trend (see Section 2.3) (Figs. 4(a) and 4(b)). The correlation coefficient between daily Dev_MDA8 O_3 and daily Dev_$PM_{2.5}$ was 0.44 (statistically significant at the 95% level).

Fig. 4 (c) shows the boxplot of Dev_MDA8 O_3 of all the O_3-polluted days occurred at the 25 sites in the YRD (Fig. 3a). With a total of 4869 samples, Dev_MDA8 O_3 concentrations were mainly in the range of 35.7 (25th percentile) to 69.5 μg m^{-3} (75th percentile) with an average value of 53.5 μg m^{-3}. Similarly, for the $PM_{2.5}$-polluted days in the YRD (Fig. 3b), with a total of 2598 samples, Dev_$PM_{2.5}$ concentrations were mainly between 22.2 (25th percentile) to 43.1 μg m^{-3} (75th percentile) with an average value of 33 μg m^{-3}. Positive Dev_MDA8 O_3 (Dev_$PM_{2.5}$) values indicate that concentrations were higher than the monthly mean values.

We pay special attention to the correlations between Dev_MDA8 O_3 and Dev_$PM_{2.5}$ for the days with Dev_MDA8 $O_3 > 0$ for April-October of 2013–2019 (Fig. S4). For most cities, the correlation coefficients were 0.2 to 0.6 (statistically significant at the 95% level), indicating positive correlations between Dev_MDA8 O_3 and Dev_$PM_{2.5}$. The positive correlation coefficients were relatively higher in Jiangsu province (cities in the eastern YRD) in the month of April, September and October and in Anhui province (cities in the western YRD) in July and August. High O_3 concentration and active photochemical reaction enhances the formation of secondary particulate matter (Wang et al., 2014; Zhu et al., 2019). The high correlations between O_3 and $PM_{2.5}$ in Jiangsu may be caused by the highest anthropogenic emissions (NO_x and NMVOCs) here compared to other regions in the YRD (Wang and Liao, 2020).

Figs. S5 shows the fraction of days with positive Dev_$PM_{2.5}$ in days with different levels of positive Dev_MDA8 O_3 in the YRD. When Dev_MDA8 O_3 were in the ranges of 0–20, 20–40, 40–60, and > 60 μg m^{-3}, the percentages of days with positive Dev_$PM_{2.5}$ were, respectively, 46.7%, 59.5%, 70.9%, and 86.4% as the percentages were averaged over

the YRD, indicating increases in percentage as Dev_MDA8 O_3 increases. When Dev_MDA8 O_3 concentrations were above 60 μg m^{-3}, the percentages of days with positive Dev_$PM_{2.5}$ in 22 cities of YRD exceeded 80%. Therefore Dev_$PM_{2.5}$ were generally positive under the conditions of high Dev_MDA8 O_3 (high levels of O_3 pollution).

3.3. Co-pollution of MDA8 O_3 and $PM_{2.5}$ in the YRD

Fig. 5 shows the scatter plot between Dev_MDA8 O_3 and Dev_$PM_{2.5}$ for all co-polluted days (days with MDA8 O_3 > 160 μg m^{-3} and $PM_{2.5}$ > 75 μg m^{-3}, Fig. 3c, a total of 654 samples) in the YRD over 2013–2019. The co-pollution occurred mainly in April (29.6%), May (23.0%), June (19.5%), and October (10.8%). The frequencies of co-pollution were small in July (6.6%), August (5.3%), and September (5.9%) owing to the low concentrations of $PM_{2.5}$ in July to September (Fig. 2c). Samples with Dev_MDA8 O_3 of 20–40, 40–60, 60–80, 80–100 μg m^{-3} had the largest contributions to the co-polluted days, which accounted for 15.1%, 28.0%, 25.7%, and 18.9% of the co-polluted days, respectively. In the co-polluted days, almost all Dev_MDA8 O_3 and Dev_$PM_{2.5}$ were positive, except very few samples with negative values due to their large monthly averaged values.

3.4. Meteorological conditions for the occurrence of co-pollution

Previous study of Li et al. (2019a) used a stepwise multiple linear regression (MLR) modeling approach to analyze NASA MERRA-2 reanalyzed data and observed O_3 concentrations. They found that changes in MDA8 O_3 concentrations in the YRD were driven by relative humidity (RH) and 10-m winds. The study by Zhu et al. (2019) found strong positive $PM_{2.5}$–O_3 correlations when air temperatures were high in summertime in southern China. Therefore, to identify the meteorological conditions for the co-pollution of O_3 and $PM_{2.5}$, we show the scatterplots of Dev_MDA8 O_3 and Dev_$PM_{2.5}$ color coded with Dev_RH (deviation of surface RH), Dev_TS (deviation of surface air temperature), and Dev_WS (deviation of surface wind speed) for days with O_3 pollution alone (i.e., MDA8 O_3 > 160 μg m^{-3} and $PM_{2.5}$ < 35 μg m^{-3}) (Fig. 6a) and for days with co-pollution of O_3 and $PM_{2.5}$ (i.e., MDA8 O_3 > 160 μg m^{-3} and $PM_{2.5}$ > 75 μg m^{-3}) (Fig. 6b). The data samples in Fig. 6 are from the 14 cities of the YRD with observed meteorological parameters available (Fig. 1), with 424 samples in Fig. 6a and 274 samples in Fig. 6b.

Compared to the meteorological conditions that O_3 pollution occurred, the co-pollution of O_3 and $PM_{2.5}$ occurred under the conditions of relatively higher RH, higher surface temperature, and lower wind speed, as summarized by Fig. 6c. The mean values of Dev_RH, Dev_TS, and Dev_WS were, respectively, −7.3%, 0.46 °C, −0.17 m s^{-1} for days with O_3 pollution alone while −6.2%, 1.84 °C, and − 0.40 m s^{-1} for days with co-pollution of O_3 and $PM_{2.5}$. Higher RH promoted hygroscopic growth of $PM_{2.5}$ components (Tie et al., 2017), higher temperature favored the formation of both O_3 and sulfate (Liao et al., 2009), and lower wind speed was not beneficial to the dilution of all pollutants.

To further understand the weather conditions under which the co-pollution of MDA8 O_3 and $PM_{2.5}$ occurred, we analyzed 33 co-polluted days in the YRD during 2013–2019. In each of these co-polluted days, over 50% of cities in the YRD experienced co-pollution. The 33 co-polluted days were classified into the months that they occurred, and the composite analysis was carried out for samples in each month (Fig. S6). Considering the similarities between weather patterns on the basis of geopotential height and winds at 850 hPa, the synoptic weather patterns for the co-pollution of O_3 and $PM_{2.5}$ in the YRD can be further classified into four types (Fig. 7). We also use the cost733class software package (http://cost733.met.no) of T-PCA to identify the weather patterns (Li et al., 2019), which obtains the same four types of synoptic weather patterns as shown in Fig. 7. The spatial distributions of concentrations of MDA8 O_3 and $PM_{2.5}$ averaged over the four types of co-polluted days are shown in Fig. S7. Type 1 was the most dominant weather pattern for co-pollution, which was associated with 22 (66.7%) of the 33 co-polluted days and occurred in April, May, and June. It was characterized by westerlies at 500 hPa over the YRD, indicating a stable weather condition without cold air intrusion from the north. At 850 hPa, the YRD was under the influence of a high pressure ridge, which was accompanied with descending air and led to dry and warm conditions at the surface (Fig. S8). Type 2 was responsible for 4 co-polluted days (12.1%) and occurred in July. With this weather pattern, the continental high in Mongolia and north China extended to the YRD at 500 hPa. At 850 hPa, a weak high was located to the north of the YRD with weak winds, which was favorable for the accumulation of O_3 and $PM_{2.5}$. Type 3 was associated with 2 (6.1%) co-polluted days that occurred in August. The Northeast Cold Vortex (NCV) at 500 hPa restricted the westward extension of the Western Pacific Subtropical High (WPSH) and the YRD was located within a uniform pressure field with very weak winds at 850 hPa. Type 4 weather pattern was associated with 5 (15.1%) co-polluted days that occurred in September and October. South China was under the control of WPSH at 500 hPa and the YRD was located in the center of a high pressure system at 850 hPa. The strong descending motion (Fig. S8) inceased surface-layer concentraions of $PM_{2.5}$ and O_3 through weakened vertical dispersion and also transported O_3 from the upper boundary layer to the surface (Gong and Liao, 2019).

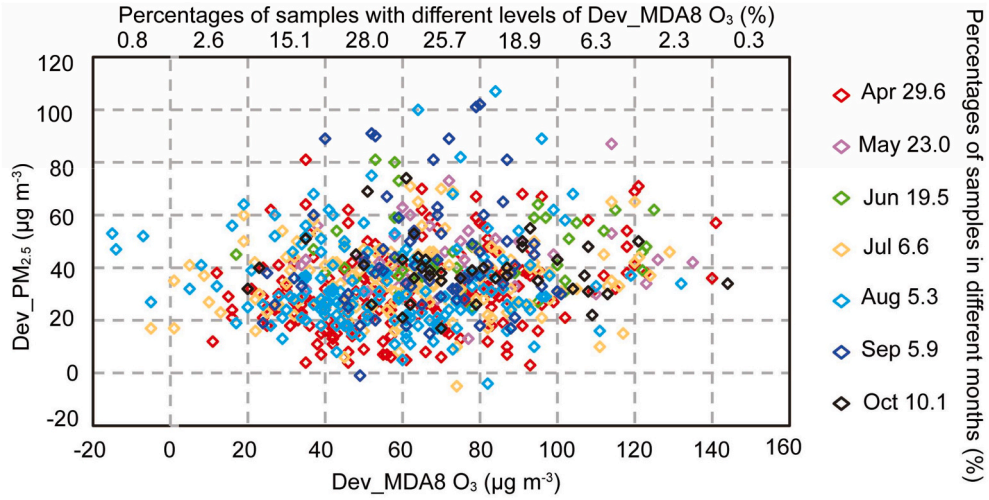

Fig. 5. The scatter plot of Dev_ MDA8 O_3 and Dev_$PM_{2.5}$ for co-polluted days in 25 cities (shown in Fig. 3c). There are 654 samples in total in April-October during 2013–2019. Percentages of samples with different levels of Dev_MDA8 O_3 and in different months are also indicated.

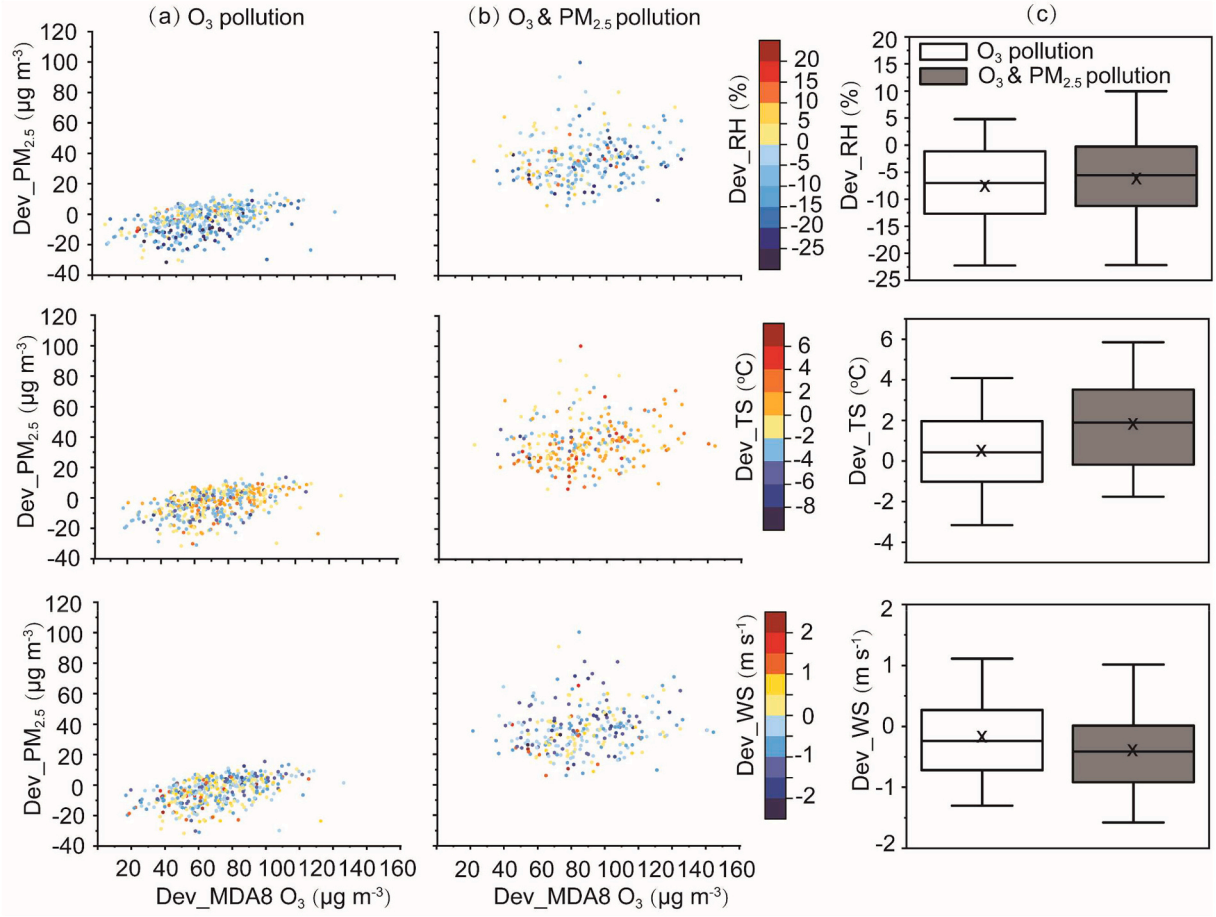

Fig. 6. Scatter plots of Dev_MDA8 O_3 and Dev_$PM_{2.5}$ color coded with Dev_RH (deviation of relative humidity, %), Dev_TS (deviation of surface temperature, °C), and Dev_WS (deviation of wind speed, m s^{-1}) for (a) days with O_3 pollution alone (MDA8 O_3 > 160 μg m^{-3} and $PM_{2.5}$ < 35 μg m^{-3}) and (b) days with co-pollution of O_3 and $PM_{2.5}$ (MDA8 O_3 > 160 μg m^{-3} and $PM_{2.5}$ > 75 μg m^{-3}). Data samples are from the 14 cities of YRD with observed meteorological parameters available. From 2013 to 2019, there were 424 samples in (a) and 274 samples in (b). (c) The boxplots of Dev_RH, Dev_TS and Dev_WS for O_3 polluted days and co-polluted days. The boxes enclose the 25th, 50th and 75th percentile, the whiskers represent the 5th and 95th percentile, the crosses represent the average values.

4. Conclusion

We investigated the simultaneous variations of O_3 and $PM_{2.5}$ in the YRD region by analyzing the observed concentrations in 25 cities from the website of Ministry of Ecological and Environment. Averaged over the YRD, the annual mean concentration of MDA8 O_3 increased by 36.8 μg m^{-3} (49.5%) whereas that of $PM_{2.5}$ decreased by 13.3 μg m^{-3} (22.1%) over 2014–2019. Considering the Grade II NAAQS for O_3 (daily MDA8 O_3 > 160 μg m^{-3}) and for $PM_{2.5}$ (daily $PM_{2.5}$ > 75 μg m^{-3}), over the studied period, provinces of Anhui had the highest frequencies of $PM_{2.5}$ polluted days (with a maximum of 708 days in city of Hefei) and provinces of Zhejiang had the highest frequencies of O_3 polluted days (with a maximum of 363 days in city of Jiaxing). The co-pollution of O_3 and $PM_{2.5}$ was also observed to occur frequently in the YRD; during 2013–2019, the co-polluted days exceeded 45 days in Shanghai and in 4 cities in Jiangsu province.

Dev_MDA8 O_3 and Dev_$PM_{2.5}$ were used to remove the trends in concentrations caused by changes in emissions and meteorology. Averaged over the YRD, daily Dev_MDA8 O_3 and daily Dev_$PM_{2.5}$ in April-October of 2013–2019 had a statistically significant correlation coefficient of 0.44. For most cities in the YRD, Dev_MDA8 O_3 and Dev_$PM_{2.5}$ exhibited positive correlations as Dev_MDA8 O_3 > 0, and the statistically significant correlation coefficients were in the range of 0.2–0.6. We found that, under the condition of Dev_MDA8 O_3 > 0, positive Dev_$PM_{2.5}$ occurred more frequently in the YRD as the value of Dev_MDA8 O_3 increased. For example, in days with Dev_MDA8 O_3 in the range of 40–60 μg m^{-3} (>60 μg m^{-3}), 59.5% (86.4%) of these days had positive Dev_$PM_{2.5}$.

We pay special attention to the days co-polluted by O_3 and $PM_{2.5}$. The co-polluted days in the YRD occurred mainly in April (29.6% of co-polluted days occurred in April), May (23.0%), June (19.5%), and October (10.8%). Compared to the days with O_3 pollution alone, the co-pollution occurred under meteorological conditions of higher relative humidity, higher surface air temperature, and lower wind speed. The mean values of Dev_RH, Dev_TS, and Dev_WS were, respectively, −7.3%, 0.46 °C, −0.17 m s^{-1} for days with O_3 pollution alone while −6.2%, 1.84 °C, and −0.40 m s^{-1} for days with co-pollution of O_3 and $PM_{2.5}$.

The synoptic weather patterns that led to the co-pollution of O_3 and $PM_{2.5}$ were classified into four types. Types 1 to 4 accounted for 66.7%, 12.1%, 6.1%, and 15.1% of the regional co-polluted days, respectively. The most dominant weather type (Type 1) occurred in April, May, and June. Over the YRD, this weather pattern was characterized by westerlies at 500 hPa (without cold air intrusion) and by a high pressure ridge at 850 hPa, leading hot, dry, and stagnant weather that was favorable for high levels of both O_3 and $PM_{2.5}$. The second most dominant weather type (Type 4) was characterized by a high pressure system over the YRD at 850 hPa, leading to strong descending motion and weakened vertical dispersion and consequently the increases in surface-layer concentrations of $PM_{2.5}$ and O_3. These two types were responsible for 81.8% (66.7% +15.1%) of the large-scale co-pollution in the YRD.

These results have important implications for the control of co-

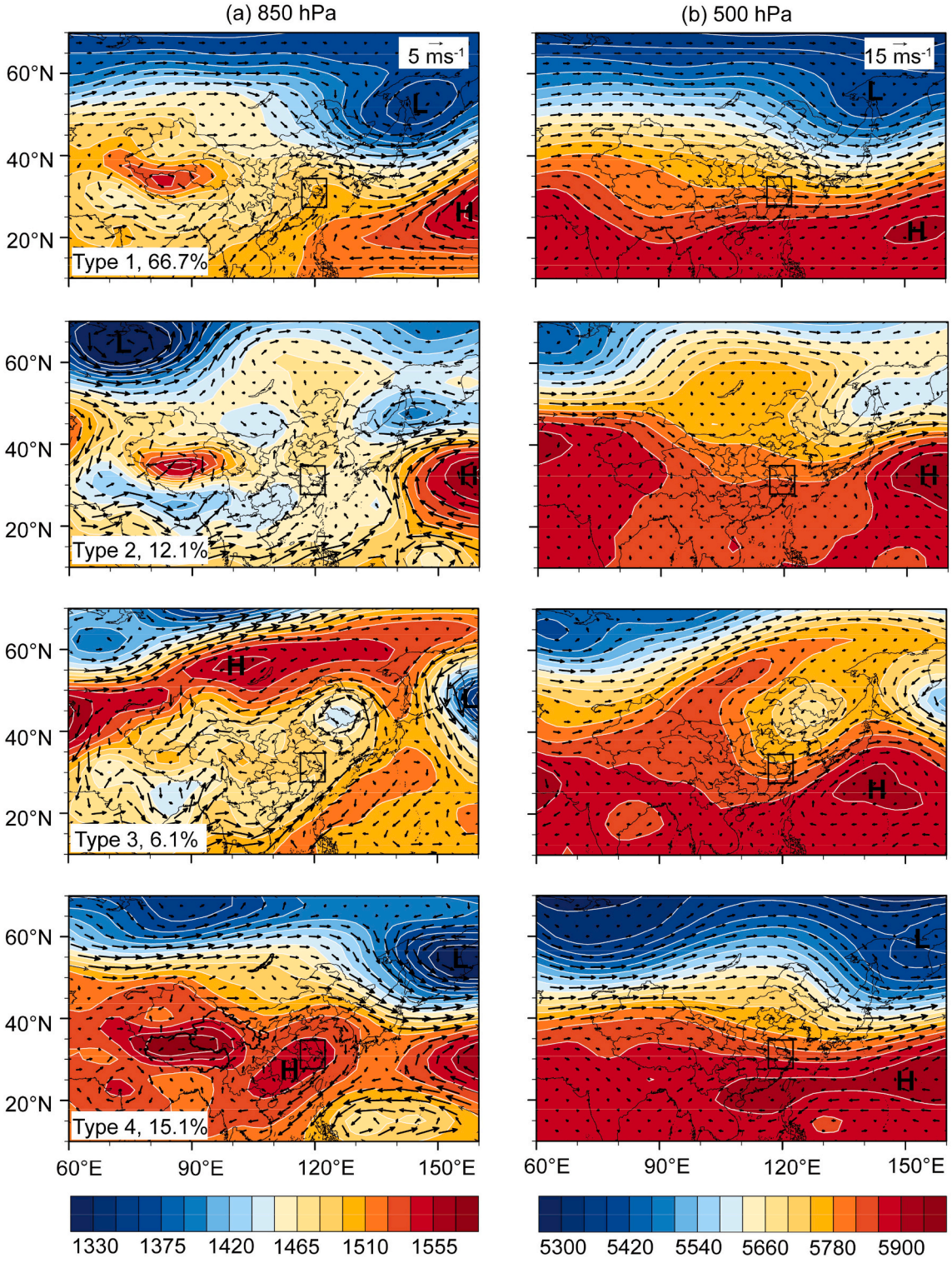

Fig. 7. Composited weather patterns for 4 types of co-polluted days in over 2013–2019. The co-polluted days were selected when over 50% of cities in YRD experienced co-pollution (MDA8 $O_3 > 160$ μg m^{-3} and $PM_{2.5} > 75$ μg m^{-3}). Black box in each panel indicates YRD. Geopotential height (m, shades) and wind vector (m s^{-1}) are shown for (a) 850 hPa and (b) 500 hPa.

polluted days in the YRD. The frequencies of the co-occurrence of O_3 and $PM_{2.5}$ pollution are higher in Jiangsu province and Shanghai than in Zhejiang and Anhui provinces during the warm months of April to October. Therefore, stringent emission control measures of NO_x and VOCs should be applied when the dominant circulation patterns of co-polluted days are predicted, especially for Jiangsu and Shanghai.

Declaration of Competing Interest

None.

Acknowledgements

This work was supported by the National Natural Science Foundation

of China (grant no. 91744311), the National Key Research and Development Program of China (grant no. 2019YFA0606804), and the College Students' Enterprise and Entreprenuership Education Program of NUIST (grant no. 201910300019Z).

Appendix A. Supplementary data

Supplementary data to this article can be found online at https://doi.org/10.1016/j.atmosres.2020.105363.

References

Cai, W., Li, K., Liao, H., Wang, H., Wu, L., 2017. Weather conditions conducive to Beijing severe haze more frequent under climate change. Nat. Clim. Chang. 7, 257–263. https://doi.org/10.1038/nclimate3249.

Ding, A., Fu, C.B., Yang, X., Sun, J., Zheng, L., Xie, Y., Herrmann, E., Nie, W., Petaja, T., Kerminen, V.-M., Kulmala, M., 2013. Ozone and fine particle in the western Yangtze River Delta: an overview of 1 yr data at the SORPES station. Atmos. Chem. Phys. 13, 5813–5830. https://doi.org/10.5194/acp-13-5813-2013.

Gao, Y., Ji, H., 2018. Microscopic morphology and seasonal variation of health effect arising from heavy metals in $PM_{2.5}$ and PM_{10}: One-year measurement in a densely populated area of urban Beijing. Atmos. Res. 212, 213–226. https://doi.org/10.1016/j.atmosres.2018.04.027.

Gong, C., Liao, H., 2019. A typical weather pattern for the ozone pollution events in North China. Atmos. Chem. Phys. 19, 13725–13740. https://doi.org/10.5194/acp-19-13725-2019.

Hou, X., Zhu, B., Kumar, R.K., Lu, W., 2019. Inter-annual variability in fine particulate matter pollution over China during 2013–2018: Role of meteorology. Atmos. Environ. 214, 116842. https://doi.org/10.1016/j.atmosenv.2019.116842.

Jiang, N., Li, L., Wang, S., Li, Q., Dong, Z., Duan, S., Zhang, R., Li, S., 2019. Variation tendency of pollution characterization, sources, and health risks of $PM_{2.5}$-bound polycyclic aromatic hydrocarbons in an emerging megacity in China: based on three-year data. Atmos. Res. 217, 81–92. https://doi.org/10.1016/j.atmosres.2018.10.023.

Li, J., Liao, H., Hu, J., Li, N., 2019. Severe particulate pollution days in China during 2013-2018 and the associated typical weather patterns in Beijing-Tianjin-Hebei and the Yangtze River Delta regions. Environ. Pollut. 248, 74–81. https://doi.org/10.1016/j.envpol.2019.01.124.

Li, K., Jacob, D.J., Liao, H., Shen, L., Zhang, Q., Bates, K.H., 2019a. Anthropogenic drivers of 2013-2017 trends in summer surface ozone in China. Proc. Natl. Acad. Sci. U. S. A. 116 (2), 422–427. https://doi.org/10.1073/pnas.1812168116.

Li, K., Jacob, D.J., Liao, H., Zhu, J., Shah, V., Shen, L., Bates, K., Zhang, Q., Zhai, S., 2019b. A two-pollutant strategy for improving ozone and particulate air quality in China. Nat. Geosci. 12, 906–910. https://doi.org/10.1038/s41561-019-0464-x.

Liao, H., Zhang, Y., Chen, W.-T., Raes, F., Seinfeld, J.H., 2009. Effect of chemistry-aerosol-climate coupling on predictions of future climate and future levels of tropospheric ozone and aerosols. J. Geophys. Res. 114, D10306 https://doi.org/10.1029/2008JD010984.

Liu, Y., Wang, T., 2020. Worsening urban ozone pollution in China from 2013 to 2017 – Part 2: the effects of emission changes and implications for multi-pollutant control. Atmos. Chem. Phys. https://doi.org/10.5194/acp-2020-53.

Liu, Y., Li, L., An, J., Huang, L., Yan, R., Huang, C., Wang, H., Wang, Q., Wang, M., Zhang, W., 2018. Estimation of biogenic VOC emissions and its impact on ozone formation over the Yangtze River Delta region, China. Atmos. Environ. 186, 113–128. https://doi.org/10.1016/j.atmosenv.2018.05.027.

Lou, S., Liao, H., Zhu, B., 2014. Impacts of aerosols on surface-layer ozone concentrations in China through heterogeneous reactions and changes in photolysis rates. Atmos. Environ. 85, 123–138. https://doi.org/10.1016/j.atmosenv.2013.12.004.

Ren, W., Tian, H., Tao, B., Chappelka, A., Sun, G., Lu, C., Liu, M., Chen, G., Xu, X., 2011. Impacts of tropospheric ozone and climate change on net primary productivity and net carbon exchange of China's forest ecosystems. Glob. Ecol. Biogeogr. 20, 391–406. https://doi.org/10.1111/j.1466-8238.2010.00606.x.

Sha, T., Ma, X., Jia, H., 2019. Exploring the influence of two inventories on simulated air pollutants during winter over the Yangtze River Delta. Atoms. Environ. 206 https://doi.org/10.1016/j.atmosenv.2019.03.006 (170–12).

Shu, L., Xie, M., Gao, D., Wang, T., Fang, D., Liu, Q., Huang, A., Peng, L., 2017. Regional severe particle pollution and its association with synoptic weather patterns in the Yangtze River Delta region, China. Atmos. Chem. Phys. 17, 12871–12891. https://doi.org/10.5194/acp-2017-473.

Sun, J., Huang, L., Liao, H., Li, J., Hu, J., 2017. Impacts of regional transport on particulate matter pollution in China: a review of methods and results. Curr. Pollut. Rep. 3, 182–191. https://doi.org/10.1007/s40726-017-0065-5.

Tai, A.P.K., Mickley, L.J., Jacob, D.J., 2010. Correlations between fine particulate matter ($PM_{2.5}$) and meteorological variables in the United States: Implications for the sensitivity of $PM_{2.5}$ to climate change. Atmos. Environ. 44, 3976–3984. https://doi.org/10.1016/j.atmosenv.2010.06.060.

Tie, X., Huang, R., Cao, J., Zhang, Q., Cheng, Y., Su, H., Chang, D., Pöschl, U., Hoffmann, T., Dusek, U., Li, G., Worsnop, D.R., O'Dowd, C.D., 2017. Severe pollution in China amplified by atmospheric moisture. Sci. Rep-UK 7 (1), 15760. https://doi.org/10.1038/s41598-017-15909-1.

Wang, Y., Liao, H., 2020. Effect of emission control measures on ozone concentrations in Hangzhou during G20 meeting in 2016. Chemosphere 261, 127729. https://doi.org/10.1016/j.chemosphere.2020.127729.

Wang, H., Kiang, C., Tang, X., Zhou, X., Chameides, W.L., 2005. Surface ozone: a likely threat to crops in Yangtze delta of China. Atmos. Eviron. 39, 3843–3850. https://doi.org/10.1016/j.atmosenv.2005.02.057.

Wang, X., Manning, W., Feng, Z., Zhu, Y., 2007. Ground-level ozone in China: distribution and effects on crop yields. Environ. Pollut. 147 (2), 394–400. https://doi.org/10.1016/j.envpol.2006.05.006.

Wang, Y., Ying, Q., Hu, J., Zhang, H., 2014. Spatial and temporal variations of six criteria air pollutants in 31 provincial capital cities in China during 2013–2014. Environ. Int. 73, 413–422. https://doi.org/10.1016/j.envint.2014.08.016.

Wang, Y., Du, H., Xu, Y., Lu, D., Wang, X., Guo, Z., 2018a. Temporal and spatial variation relationship and influence factors on surface urban heat island and ozone pollution in the Yangtze River Delta, China. Sci. Total Environ. 631-632, 921–933. https://doi.org/10.1016/j.scitotenv.2018.03.050.

Wang, J., Zhang, X., Li, D., Yang, Y., Zhong, J., Wang, Y., Che, H., Che, H., Zhang, Y., 2018b. Interdecadal changes of summer aerosol pollution in the Yangtze River Basin of China, the relative influence of meteorological conditions and the relation to climate change. Sci. Total Environ. 630, 46–52. https://doi.org/10.1016/j.scitotenv.2018.01.236.

Xie, Y., Dai, H., Zhang, Y., Wu, Y., Hanaoka, T., Masui, T., 2019. Comparison of health and economic impacts of $PM_{2.5}$ and ozone pollution in China. Environ. Int. 130, 104881. https://doi.org/10.1016/j.envint.2019.05.075.

Xu, X., Lin, W., Wang, T., Yan, P., Tang, J., Meng, Z., Wang, Y., 2008. Long-term trend of surface ozone at a regional background station in eastern China 1991–2006: enhanced variability. Atmos. Chem. Phys. 8, 2595–2607. https://doi.org/10.5194/acpd-8-215-2008.

Xue, L., Wang, T., Gao, J., Ding, A., Zhou, X., Blake, D., Wang, X., Saunders, S.M., Fan, S. J., Zuo, H., Zhang, Q., Wang, W., 2014. Ground-level ozone in four Chinese cities: precursors, regional transport and heterogeneous processes. Atmos. Chem. Phys. 14, 13175–13188. https://doi.org/10.5194/acp-14-13175-2014.

Yu, Y., Wang, Z., He, T., Meng, X., Xie, S., Yu, H., 2019. Driving factors of the significant increase in surface ozone in the Yangtze River Delta, China, during 2013–2017. Atoms. Pollut. Res. 10, 1357–1364. https://doi.org/10.1016/j.apr.2019.03.010.

Yue, X., Unger, N., Harper, K., Xia, X., Liao, H., Zhu, T., Xiao, J., Feng, Z., Li, J., 2017. Ozone and haze pollution weakens net primary productivity in China. Atmos. Chem. Phys. 17, 6073–6089. https://doi.org/10.5194/acp-2016-1025.

Zhang, N., Ma, F., Qin, C.B., Li, Y.F., 2018a. Spatiotemporal trends in $PM_{2.5}$ levels from 2013 to 2017 and regional demarcations for joint prevention and control of atmospheric pollution in China. Chemosphere 210, 1176–1184. https://doi.org/10.1016/j.chemosphere.2018.07.142.

Zhang, Q., Ma, Q., Zhao, B., Liu, X., Wang, Y., Jia, B., Zhang, X., 2018b. Winter haze over North China Plain from 2009 to 2016: influence of emission and meteorology. Environ. Pollut. 242, 1308–1318. https://doi.org/10.1016/j.envpol.2018.08.019.

Zhu, J., Chen, L., Liao, H., Dang, R., 2019. Correlations between $PM_{2.5}$ and ozone over China and associated underlying reasons. Atmosphere 10, 352. https://doi.org/10.3390/atmos10070352.

Stocker, T.F., Qin, D., Plattner, G.-K., Tignor, M., Allen, S.K., Boschung, J., Nauels, A., Xia, Y., Bex, V., Midgley, P.M. (Eds.), 2013. IPCC, 2013: Climate Change 2013: The Physical Science Basis. Contribution of Working Group I to the Fifth Assessment Report of the Intergovernmental Panel on Climate Change. Cambridge University Press, Cambridge, United Kingdom and New York, PP. 1535.